JCSE The Journal of Corrosion Science and Engineering

21st Century Corrosion Science

Volume 6 Paper C016

Potential Dependence of Frictional Coefficient Evaluated by *In-situ* Nano-scratching for the Passive Iron Surface

Makoto Chiba and Masahiro Seo

Graduate School of Engineering, Hokkaido University, Kita-13Jo, Nishi-8Chome, Kita-ku, Sapporo 060-8628, Japan,

chiba@elechem1-mc.eng.hokudai.ac.jp

Abstract

In-situ (kept potentiostatically in the passive state) and *ex-situ* (in air after passivation) nano-scratching tests were performed to the iron single crystal (100) surfaces passivated at 0.0 V – 1.0 V (SHE) in pH 8.4 borate solution to evaluate the friction coefficient of the passive surface and its potential dependence. The friction coefficient obtained with *in-situ* nano-scratching for the passive iron (100) surface was significantly larger than that obtained with *ex-situ* nano-scratching. The friction coefficient obtained with *ex-situ* nano-scratching was almost independent of potential in the passive region. On the other hand, the friction coefficient obtained with *in-situ* nano-scratching increased with increasing potential in the passive region. These results were explained in terms of a series of mechano-electrochemical reaction such as the film rupture, active dissolution and repassivation taking place at the moving front of the indenter during *in-situ* nano-scratching.

Keywords: Nano-scratching test, Friction coefficient, Single crystal iron, Passive film

Introduction

There have been many studies of passive films on metals. Most of studies reported so far were focused on the chemical properties [1-13] such as composition, structure and thickness of passive film, or semiconductive properties, while there were few studies on mechanical properties of passive films on metals. Recently it has been reported that the chemical or electrochemical properties of passive metal surfaces correlate their mechanical properties to some extent [14-19]. If the correlation between chemical or electrochemical and mechanical properties is made clear, the mechano-electrochemical knowledge valuable for better understanding of the passivity breakdown and repassivation will be acquired.

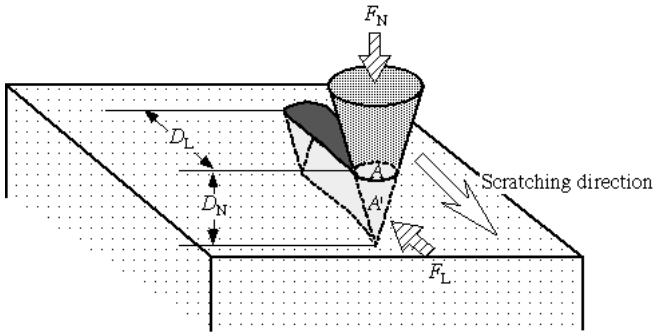

Fig. 1 Outline of nano-scratching process.

F_N: normal force
F_L: lateral force
D_N: normal displacement
D_L: lateral displacement
A : horizontal cross sectional area of the indenter tip in contact with the surface
A' : vertical cross sectional area of the indenter tip in contact with the surface

The recent development of nano-indentation or nano-scratching technique has made feasible to evaluate the mechanical properties of surface thin films on solids such as hardness, elastic modulus or friction coefficient [20-25]. In our previous studies [15,17-19], the first attempt of *in-situ* nano-indentation and *in-situ* nano-scratching in solution to the single crystal iron surfaces as kept at a constant potential in the passive region succeeded in getting the substantial information regarding the nano-mechano-electrochemical properties of the passive surfaces.

In this study, *in-situ* (kept potentiostatically in the passive state) and *ex-situ* (in air after passivation) nano-scratching techniques were applied to the single crystal iron (100) surfaces passivated at various

potentials in pH 8.4 borate solution to evaluate the friction coefficient of the passive iron surface and its potential dependence.

Experimental

Single crystal iron (100) disk-plate with a diameter of 10 mm and a thickness of 1.4 mm were used for experiments. The iron specimen was mechanically polished and then finally electropolished with a constant current density of 32 mA cm^{-2} in a mixture of 70 % $HClO_4$ and glacial CH_3COOH (1 : 20) at 17 °C. The electrolyte solution employed for passivation was pH 8.4 borate solution. The passivation of the iron specimen was performed with a potentiostatic polarization at 0.0 V – 1.0 V (SHE) for 1 h in pH 8.4 borate solution, after cathodic reduction of an air-formed film at a constant current density of –30 μA cm^{-2} for 10 min. A small electrochemical cell made from Diflon was specially designed for *in-situ* nano-scratching test in solution. Platinum ring and wire were used as counter and reference electrodes, respectively.

The transducer (Hysitron Co. Ltd., Triboscope) for nano-scratching was combined with AFM (Digital Instruments, Nanoscope IIIa) in which the electrochemical cell was set. Normal and lateral forces (F_N and F_L), and normal and lateral displacements (D_N and D_L) can be measured simultaneously by using this transducer. The iron specimen was potenstatically passivated at various potentials in the passive region for 1 h in pH 8.4 borate solution at 25 °C. The *in-situ* nano-scratching was performed on the specimen surface kept at the same passive potential in pH 8.4 borate solution after passivation for 1 h. The *ex-*

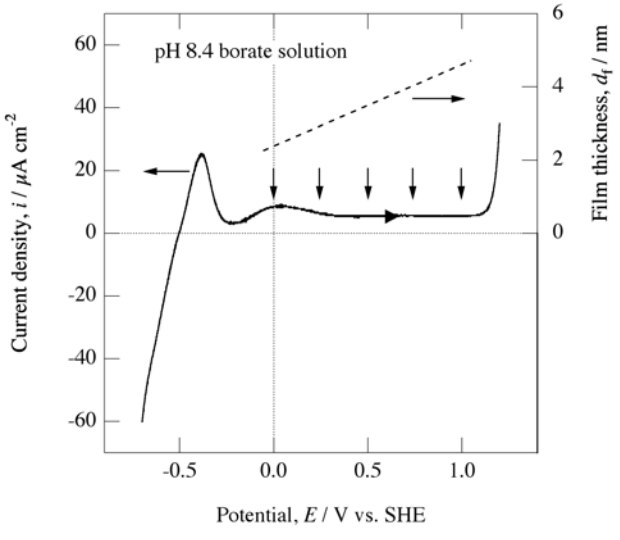

Fig. 2 Potentiodynamic polarization curve of the iron (100) surface measured with a potential sweep rate of 100 mV min^{-1} in pH 8.4 borate solution.
The dashed line represents the thickness, d_f, of passive film on iron obtained ellipsometrically by Sato *et al.*[2].

situ nano-scratching was also performed on the specimen taken out from the solution in air after passivation, washed with milli-Q filtered water and dried with a jet of nitrogen gas. A conical diamond indenter with a tip radius less than 1 μm and an included angle of 90 degree was employed for nano-scratching and attached to a tungsten rod for use in liquid. After nano-scratching test, the morphology of the scratched area can be observed with AFM by using the same tip used for nano-scratching.

Figure 1 shows the outline of nano-scratching process. At first, the tip was indented to the sample surface by a normal force, F_N, in the range of 100 – 1000 μN and then the tip was moved to the lateral direction under the constant normal force for 10 s at a scratching rate of 0.2 μm s^{-1} between a distance of 2 μm to obtain a lateral force, F_L, and a normal displacement, D_N, respectively, as a function of lateral displacement, D_L. The friction coefficient, μ', is defined with dividing a lateral force, F_L, by a normal force, F_N, [26] as represented by Eq. (1).

$$\mu' = F_L / F_N \qquad (1)$$

Results and Discussion

Figure 2 shows the potentiodynamic anodic polarization curve of the iron (100) surface measured with a potential sweep rate of 100 mV min^{-1} in pH 8.4 borate solution. The vertical arrows in Fig. 2 represent the potentials at which the nano-scratching tests were performed. According to the ellipsometrical results by Sato *et al.* [2], the thickness of passive film formed potentiostatically on a polycrystalline iron surface for 1 h in pH 8.4 borate solution increases linearly with film formation potential and is in the range of 2 – 5 nm as shown in a dashed line of Fig. 2.

Figure 3 shows the normal displacement, D_N, and friction coefficient, μ', as a function of lateral displacement, D_L, obtained with *in-situ* (kept at 0.25 V) nano-scratching at a normal force of F_N = 500 μN for the iron (100) surface passivated at 0.25 V (SHE) for 1 h in pH 8.4 borate solution. The normal displacement, D_N, increases with increasing lateral displacement, D_L, passing through a maximum, and

attains a steady state. On the other hand, the friction coefficient, μ', increases monotonously with increasing lateral displacement, D_L, and attains a steady state. In the steady state region where the friction coefficient is independent of the lateral displacement, the friction coefficient is insensitive to the change in the normal displacement. Here, the steady state value of friction coefficient was employed for discussion.

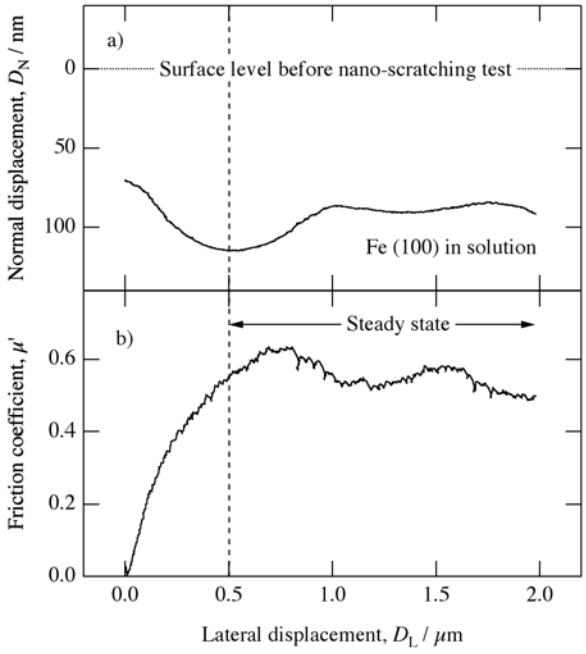

Fig. 3 a) Normal displacement, D_N, and b) friction coefficient, μ', as a function of lateral displacement, D_L, obtained with *in-situ* nano-scratching at a normal force, $F_N = 500\ \mu$N for the iron (100) surface passivated at 0.25 V (SHE) for 1 h in pH 8.4 borate solution.

Figure 4 shows the AFM image and the height-profile of the scratched area for the passive iron (100) surface after *in-situ* nano-scratching test. The groove produced by the scratching and the resultant protrusion can be observed clearly from the AFM image. From the height-profile along the dashed line in the AFM image of Fig. 4, it is seen that the depth of the groove, D_G, is 50 – 100 nm, which is less than the normal displacement, D_N, of 70 – 120 nm in Fig. 3 a). This difference between D_G and D_N may be ascribed to the contribution of elastic deformation to D_N, since D_N contains both contributions of elastic and plastic deformation, while D_G after the scratching contains only the contribution of plastic deformation. Furthermore, as seen from the comparison between Fig. 3 a) and Fig. 4 b), the lateral changes of D_G are less than the changes of D_N with D_L, which may be caused by the size effect of the tip because the tip radius (< 1 μm) is not sufficiently small to measure exactly the bottom depth of the groove.

Figure 5 shows the friction coefficient, μ', as a function of normal force, F_N, obtained with *in-situ* and *ex-situ* nano-scratching tests to the iron (100) surfaces passivated at 0.25 V and 0.75 V (SHE) for 1 h in pH 8.4 borate solution. Here, these friction coefficients were obtained by averaging the values measured 10-20 times at each normal force and their standard deviations were 25%. A single crystal may exhibit non-isotropic deformation behavior which would provide the dependence of friction coefficient on scratching direction. In the present nano-scratching tests, the scratching direction was not specified. The effects of scratching direction on friction coefficient, even they are present, might be masked in the standard deviation of 25 %. The friction coefficients obtained with *in-situ* nano-scratching are independent of normal force within the standard deviation of 25 %, while the friction coefficients, μ', obtained with *ex-situ* nano-scratching increase with increasing normal force, F_N. It should be noted that the friction coefficients of the iron (100) surfaces obtained with *in-situ* nano-scratching test are larger than those obtained with *ex-situ* nano-scratching test. Moreover, the friction coefficient of the iron (100) surface passivated at 0.75 V obtained by *in-situ* nano-scratching test is larger than that of the iron (100) surface passivated at 0.25 V. In contrast, there is no significant difference between the friction coefficient of the iron (100) surface passivated 0.25 V and 0.75 V obtained with *ex-situ* nano-scratching test.

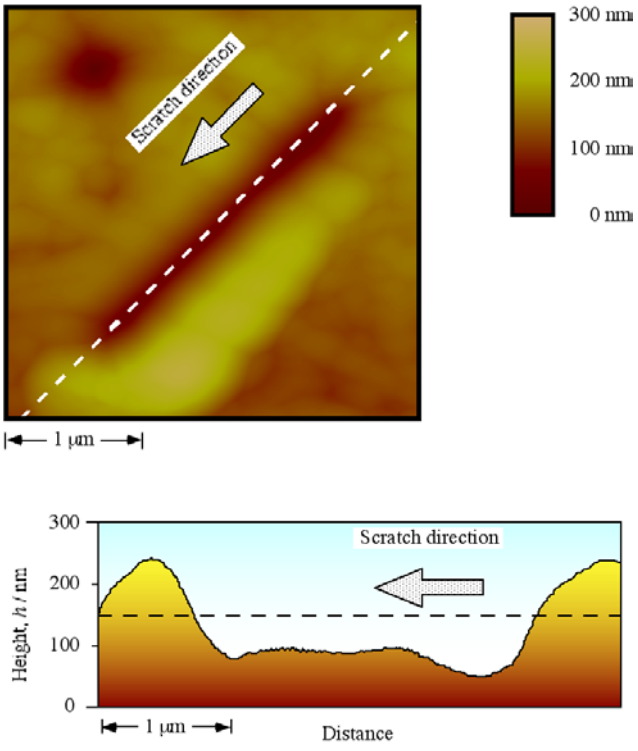

Fig. 4 a) AFM image of the passive iron (100) surface after *in-situ* nano-scratching test and b) height-profile of the scratched area along the dashed line in the AFM image.

In Figs. 6 and 7, the friction coefficients, μ', obtained with *in-situ* and *ex-situ* nano-scratching tests under the normal forces, F_N = 100 μN and 1000 μN are plotted as a function of potential for the iron (100) surface passivated at various potentials, E. The friction coefficients obtained with *in-situ* nano-scratching test increase with increasing potential, while those obtained with *ex-situ* nano-scratching have no significant potential dependence. The potential dependence (0.24 V^{-1}) of the friction coefficient obtained with *in-situ* nano-scratching under F_N = 100 μN is larger than that (0.18 V^{-1}) under F_N = 1000 μN. The normal displacements, D_N, under F_N = 100 μN and 1000 μN are 30 nm and 150 nm, respectively, irrespective of *in-situ* and *ex-situ* nano-scratching, which are much larger than the thickness (2 – 5 nm) of passive films as seen from the dashed line in Fig. 2. This means that the thickness of passive film does not significantly affect the friction coefficient, which is consistent with the no significant potential dependence of the friction coefficients obtained with *ex-situ* nano-scratching. In contrast, it seems difficult to explain the significant potential dependence of the friction coefficient obtained with *in-situ* nano-scratching without taking into account a series of mechano-electrochemical reaction which would take place at the moving front of the indenter tip during *in-situ* nano-scratching as discussed later.

It is generally accepted that the lateral force, F_L, consists of the adhesion term, F_a, and the ploughing term, F_p [26].

$$F_L = F_a + F_p \qquad (2)$$

The adhesion term, F_a, is given by

$$F_a = sA \qquad (3),$$

where A is the horizontal cross sectional area of the conical indenter tip in contact with the sample surface (see Fig. 1) and s is the shear strength at the scratched interface. Hardness of material surface, H, is defined with dividing F_N by A [20].

$$H = F_N / A \qquad (4)$$

By substituting Eq. (4) into Eq. (3), the adhesion term, F_a, is represented as follows.

$$F_a = s\,(F_N / H) \qquad (5)$$

The contribution of the adhesion term to the friction coefficient, μ'_a, therefore, is given by

$$\mu'_a = s / H \qquad (6).$$

The ploughing term, F_p, is represented by

$$F_p = A'\, p_f \qquad (7),$$

where A' is the vertical cross sectional area of the conical indenter tip in contact with the sample surface (see Fig. 1) and p_f is the plastic flow pressure of materials against nano-scratching. The proportional relation holds between A and A' from the geometry of a conical indenter. If the conical indenter has an ideal geometry ($\varnothing = 45^\circ$), the proportional constant is $k = A' / A = (\cot \varnothing) / \pi = 0.318$ [26]. The ploughing term, F_p, therefore, can be replaced by

$$F_p = k A\, p_f \qquad (8).$$

By substituting Eq. (4) into Eq. (8), the ploughing term can be represented as follows.

$$F_p = (k\, p_f / H)\, F_N \qquad (9)$$

The contribution of the ploughing term to the friction coefficient, μ'_p, is eventually given by

$$\mu'_p = k\, p_f / H \qquad (10).$$

The net friction coefficient, μ', containing both contributions of adhesion and ploughing terms is eventually represented by

$$\mu' = \mu'_a + \mu'_p = s / H + k\, p_f / H \qquad (11).$$

For a single crystal iron, the value of s is less than 100 MPa at room temperature [27] and the value of H obtained with nano-indentation is about 3 GPa [17], from which μ'_a is estimated to be less

than 0.033. Assuming that p_f is equivalent to H [26], $\mu'_p = 0.318$ is estimated from Eq. (10). The net value of μ' is 0.35, which is close to the experimental values obtained with *ex-situ* nano-scratching in the range of $F_N < 300$ μN for the passive iron (100) surface. The experimental value, however, deviates upward from the estimated value with increasing F_N in the range of $F_N > 300$ μN. The dependence of μ' on F_N suggests that p_f is not equivalent to H for the passive iron surface.

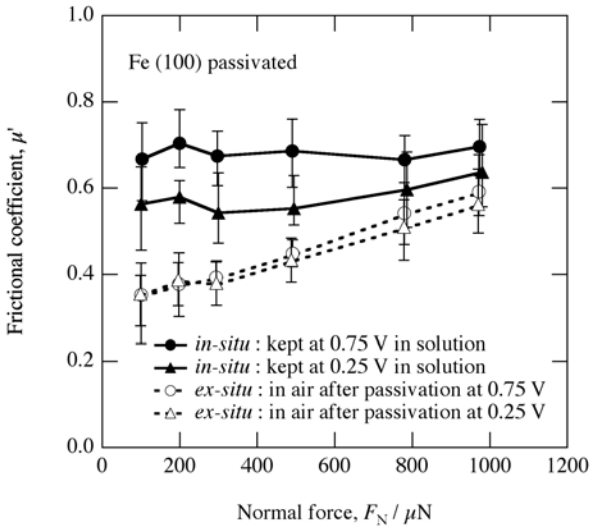

Fig. 5 Relation between friction coefficient, μ', and normal force, F_N, obtained with *in-situ* or *ex-situ* nano-scratching for the Fe (100) surfaces passivated at 0.25 V and 0.75 V (SHE).

It has been considered so far [26] that the plastic flow pressure, p_f, is peculiar to materials, *i.e.*, independent of the normal force, F_N. It is deduced from the present results that the plastic flow pressure, p_f, against nano-scratching does not only depend on materials themselves but also the normal force, F_N. Furthermore, the experimental values of μ' obtained with *in-situ* nano-scratching are significantly larger than those obtained with *ex-situ* nano-scratching, which could not be explained without taking into consideration a series of mechano-electrochemical reaction (such as the film rupture, active dissolution from the rupture sites and the repassivation) taking place at the moving front of the indenter tip during *in-situ* nano-scratching. Since the normal displacement, D_N, is significantly larger than the thickness of passive film, the

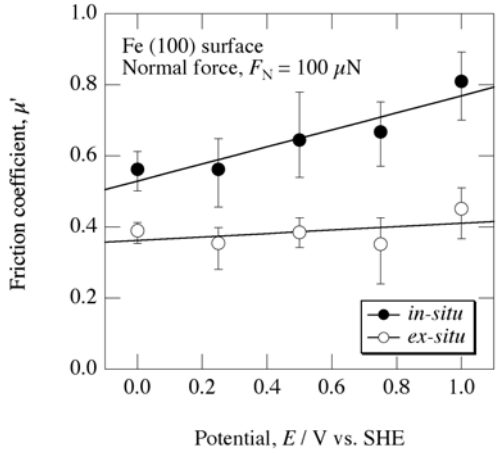

Fig. 6 Potential dependence of friction coefficient, μ', obtained with *in-situ* or *ex-situ* nano-scratching under the normal force, $F_N = 100$ μN for the passive iron (100) surface.

passive film is ruptured at the moving front of the indenter tip during nano-scratching. In case of *ex-situ* nano-scratching, the rupture sites of passive film would be repaired by air-oxidation. On the other hand, in case of *in-situ* nano-scratching, active dissolution from the rupture sites and followed by the repassivation would take place. The repassivation may be promoted by a potential difference between the iron substrate at the rupture sites and solution. The repassivation rate, therefore, increases with increasing film formation potential. The pile up of the passive film due to repassivation would provide the high impedance against the movement of the indenter tip to increase the friction coefficient. The significant potential dependence of the friction coefficient obtained with *in-situ* nano-scratching may be explained by the increase in repassivation rate due to the increase in the potential difference between the iron substrate and solution. No significant potential dependence of the friction coefficient obtained with *ex-situ* nano-scratching may be explained by the constant repassivation rate due to air oxidation. At present, there is no appropriate explanation for the potential dependence of friction coefficient obtained with *in-situ* nano-scratching except for the assumption that a series of mechano-electrochemical reaction such as film rupture, active dissolution from the rupture sites and the repassivation takes place at the moving front of the indenter tip.

Conclusions

The following conclusions were drawn from the *in-situ* and *ex-situ* nano-scratching tests for the iron (100) surface passivated at 0.0 V – 1.0 V (SHE) for 1 h pH 8.4 borate solution.

1) The friction coefficient obtained with *in-situ* nano-scratching for the passive iron (100) surface was always larger than that of obtained with *ex-situ* nano-scratching.

2) The friction coefficient of the passive iron (100) surface obtained with *in-situ* nano-scratching increased with increasing the passive film formation potential. In contrast, the friction coefficient obtained with *ex-situ* nano-scratching had no significant potential

dependence. It has been proposed that a series of mechano-electrochemical reaction (film rupture, active dissolution and repassivation) takes place at the moving front of the indenter during *in-situ* nano-scratching in order to explain the large friction coefficient obtained with *in-situ* nano-scratching.

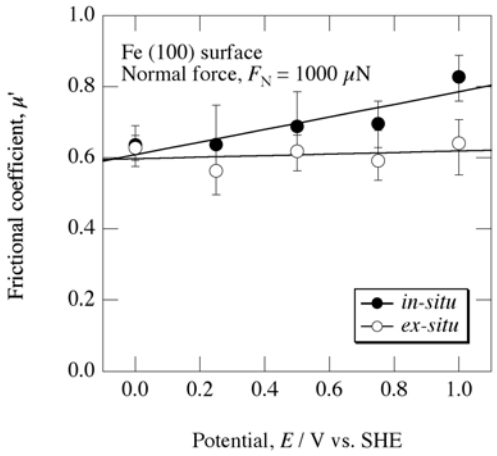

Fig. 7 Potential dependence of friction coefficient, μ', obtained with *in-situ* or *ex-situ* nano-scratching under the normal force, F_N = 1000 μN for the passive iron (100) surface.

Acknowledgement

This work was supported by a Grant-in-Aid for Scientific Research from the Ministry of Education, Science, Sport, and Culture, Japan (No. 13450288).

References

1. M. Nagayama and M. Cohen, *J. Electrochem. Soc.,* **109**, pp781-790, 1962.

2. N. Sato, K. Kudo and T. Noda, *Electrochim. Acta*, **16**, pp1909-1921, 1971.

3. J. W. Schultze and U. Stimming, *Z. Phys. Chem. N. F.*, **98**, pp285-302, 1975.

4. N. Sato, *J. Electrochem. Soc.*, **123**, pp1197-1199, 1976.

5. M. Seo and N. Sato, J. B. Lumsden and R. W. Staehle, *Corros. Sci.*, **17**, pp209-217, 1977.

6. M. Sakashita and N. Sato, *Corrosion*, **35**, pp351-355, 1979.

7. C. Y. Chao, L. F. Lin and D. D. Macdonald, *J. Electrochem. Soc.*, **128**, pp1187-1194, 1981.

8. B. D. Cahan and C.-T. Chen, *J. Electrochem. Soc.*, **129**, pp921-925, 1982.

9. N. Sato, *Corrosion*, **45**, pp354-368, 1989.

10. A. J. Davenport and M. Sansone, *J. Electrochem. Soc.*, **142**, pp725-730, 1995.

11. L. J. Oblonsky, A. J. Davenport, M. P. Ryan, H. S. Isaacs and R. C. Newman, *J. Electrochem. Soc.*, **144**, pp2398-2404, 1997.

12. M. Büchler, P. Schmuki and H. Böhni, *J. Electrochem. Soc.*, **145**, pp609-614, 1998.

13. A. J. Davenport, L. J. Oblonsky, M. P. Ryan and M. F. Toney, *J. Electrochem. Soc.,* **147**, pp2162-2173, 2000.

14. S. Mischler, A. Spiegel and D. Landolt, *Wear*, **225-229**, pp1078-1087, 1999.

15. M. Seo, M. Chiba and K. Suzuki, *J. Electroanal. Chem.*, **473**, pp49-53, 1999.

16. D. Landolt, S. Mischler and M. Stemp, *Electrochim. Acta,* **46**, pp3913-3929, 2001.

17. M. Seo and M. Chiba, *Electrochim. Acta*, **47**, pp319-325, 2001.

18. M. Chiba and M. Seo, *Corrosion Science*, **44**, pp2379-2391, 2002.

19. M. Chiba and M. Seo, *J. Electrochem. Soc.*, submitted

20. W. C. Oliver and G. M. Pharr, *J. Mater. Res.,* **7**, pp1564-1583, 1992.

21. B. Bhushan (Ed.), Handbook of Micro / Nano Tribology, CRC Press, New York, 1995.

22. S. E. Harvey, H. Huang, S. K. Venkataraman and W. W. Gerberich, *J. Mater. Res.*, **8**, pp1291-1299, 1993.

23. N. A. Stekmashenko, M. G. Walls, L. M. Brown and Yu. V. Milman, *Acta Metall. Mater.*, **41**, pp2855-2865, 1993.

24. W. W. Gerberich, S. K. Venkataraman, H. Huang, S. E. Harvey and D. L. Kohlstedt, *Acta Metall. Mater.*, **43**, pp1569-1576, 1995.

25. W. D. Nix, *Mater. Sci. Eng.*, **A 234-236**, pp37-44, 1997.

26. D. F. Moore, Principles and Applications of Tribology, Pergamon Press, Oxford, 1975.

27. Y. Aono, E. Kuramoto and K. Kitajima, Rep. Res. Inst. Appl. Mech., Kyushu Univ. XXIX, pp127-193, 1981.